



# Effects of temperature and host plant fragmentation on *Lymantria dispar* population growth along its expanding population front

Riley Metz · Patrick C. Tobin 

Received: 1 July 2021 / Accepted: 14 April 2022 / Published online: 4 May 2022  
© The Author(s), under exclusive licence to Springer Nature Switzerland AG 2022

**Abstract** *Lymantria dispar* (L.), formerly known in the U.S.A. as the gypsy moth, has been a major pest species in North American forests for > 100 years. Due to the economic and ecological consequences of *L. dispar* outbreaks, many aspects of its population biology and ecology have been studied. However, as *L. dispar* continues to spread into new areas, it remains important to understand its invasion dynamics in newly established populations where prior research is lacking. In this study, we used a 16-year spatially-referenced dataset to quantify the spatial dynamics of *L. dispar* population growth rates along its expanding population front from Minnesota to North Carolina. We then used this information in a spatially-explicit modeling framework to quantify the role of temperatures, primary and secondary *L. dispar* host plant density, and the fragmentation of primary and secondary host plants, on *L. dispar* population growth rates. Across the invasion front, temperatures were significant predictors of growth rates. The basal area of host plants, often used to predict *L. dispar* risk, was not a significant predictor in any region along the invasion front. Instead, primary and

secondary host plant cohesion (i.e., reduced fragmentation), were significant predictors of growth rates, with the exception of areas where host plants are generally scarce. The results highlight geographical differences in how temperature and host plant fragmentation affect *L. dispar* growth rates, and underscore the role that secondary host plants can play in establishing populations. The results inform the development of improved risk models of *L. dispar* invasion.

**Keywords** Climate · Generalized additive models · Growth rate · Host plant fragmentation · *Lymantria dispar* · Risk model

## Introduction

The successful establishment of non-native insect herbivores depends, in part, upon climatic suitability and the availability of host plants in the introduced range. As poikilotherms, insects are directly affected by temperatures, which can affect overwintering strategies and immature development (Sharpe and DeMichele 1977; Tauber et al. 1986). Not surprisingly, physiological restraints to temperature play an important role in determining the distributional ranges of invading and native insects (Bale et al. 2002; Jepsen et al. 2008; Tobin et al. 2014b). With temperatures projected to increase due to anthropogenic climate change, many species are expected to experience changes in their distributional ranges (Hill et al. 2011;

---

**Supplementary Information** The online version contains supplementary material available at <https://doi.org/10.1007/s10530-022-02804-8>.

---

R. Metz · P. C. Tobin (✉)  
School of Environmental and Forest Sciences, University of Washington, Seattle, WA, USA  
e-mail: pctobin@uw.edu

Weed et al. 2013). Past work on the response of individual forest insects to climate change has revealed variable responses that range from intensification in outbreaks and range expansion, to outbreak collapse and range retraction (Esper et al. 2007; Haynes et al. 2014; Logan et al. 2003; Tobin et al. 2014a). It remains integral to understand the effect that climate will have on insects, especially for invading species that cause ecological and economic damage.

The geographic ranges and population density of insect herbivores are also dependent on the availability and quality of host plants upon which they depend (Collinge 2000; Hunter 2002). Immigration to and emigration from habitat patches can also be affected by patch size and their spatial distribution across the landscape (Connor et al. 2000; Cronin 2003). Patches with greater host plant area typically yield higher population densities (Denno et al. 1981), and patch connectivity is a critical factor that affects patch occupancy and the regional dynamics of insect populations (Hanski 1998; Hanski and Gilpin 1991).

Upon successful establishment, non-native insect herbivores spread into new areas, often through stratified diffusion in which new colonies are formed by both short- and long-range dispersal events (Hengeveld 1989; Liebhold and Tobin 2008; Shigesada et al. 1995). Understanding the interplay between climate and host plant availability in an invading species can inform management plans. However, tracking an invading species at the low densities typical in newly established colonies is not trivial due to a lack of sensitive detection tools and a comprehensive monitoring network. The invasion of the European strain of *Lymantria dispar* (L.) in the United States is an exception in that its invasion along an expanding population front has been extensively monitored under the Slow-the-Spread program (Grayson and Johnson 2018; Tobin and Blackburn 2007).

Since its introduction in 1869, *L. dispar* has established in the eastern and Midwestern United States (Tobin et al. 2012), or roughly one third of its potential habitat in the United States (Morin et al. 2005), and continues to spread. Its rate of spread varies through time and space, and is believed to fluctuate as a function of variation in host availability, frequency of human transport, federal management, and Allee effects (Biggs et al. 2011; Contarini et al. 2009; Hajek and Tobin 2009; Johnson et al. 2006; Liebhold et al. 1992; Liebhold and Tobin 2006; Tobin

et al. 2007b). Because of the economic and ecological consequences of *L. dispar* invasion (Doane and McManus 1981; Elkinton and Liebhold 1990; Tobin et al. 2012), many aspects of its population biology and ecology have been studied. This includes the relationship between *L. dispar* invasion potential and climate (Allen et al. 1993; Gray 2004; Logan et al. 2007; Pitt et al. 2007) and the relationship between *L. dispar* outbreaks and the density of preferred host plants (Haynes et al. 2009; Herrick and Gansner 1986; Liebhold et al. 1994).

Populations of *L. dispar* are constrained by sub-optimal and supraoptimal temperatures. While exposure to cold temperatures is a requirement to terminate diapause, exposure to temperatures  $< -22$  °C for extended periods increases mortality (Gray 2009). Furthermore, the supercooling point in overwintering egg masses has been estimated at  $-28$  °C (Doane and McManus 1981). Supraoptimal temperatures during immature development can also affect *L. dispar* populations. For example, Tobin et al. (2014a) reported on range retraction in response to supraoptimal temperatures during spring–summer larval feeding. Thompson et al. (2017) found that extended exposure to supraoptimal temperatures affected both the larval mass and developmental time to 4<sup>th</sup> instar, and reported a lethal supraoptimal temperature of  $\sim 32$  °C.

Despite the breadth of *L. dispar* host species (Elkinton and Liebhold 1990; Liebhold et al. 1995), there can be considerable spatial variation in defoliation throughout the eastern United States, which is thought to be a result of *L. dispar* preferential feeding (Liebhold et al. 1994). Although larvae are polyphagous folivores that can feed on  $> 300$  host plant species in the United States, 146 species are considered as primary host plants (Liebhold et al. 1995), and only a portion of primary host plants are likely to be present in a specific area of invasion. Larval feeding can be divided into two phases: early larval feeding (instars 1 to 3), and late larval feeding (instars 4 to 5/6). Early larval feeding is initiated in the spring following egg hatch, which typically extends over three weeks (Stoyenoff et al. 1994). Early instars have more dietary limitations relative to late instars because the former are not metabolically adapted to host plant defensive compounds (Barbosa and Greenblatt 1979; Barbosa and Krischik 1987), which can reduce survivorship and larval weight, and increase developmental time (Miller and Feeny 1983). Consequently,

*L. dispar* host plants can be broadly divided into primary or secondary hosts. Primary hosts support *L. dispar* larval development with minimal, if any, costs to fitness, while secondary hosts can generally only be consumed by later instars. Although primary hosts have received more attention in *L. dispar* population dynamics given that a sufficient quantity of primary hosts is needed to support the development of outbreaks (Herrick and Gansner 1986; Liebhold et al. 1994; Haynes et al. 2009), scant attention has been given to the potential role of secondary host species in supporting expanding, low-density *L. dispar* populations. Moreover, it is not known if suboptimal and supraoptimal temperatures interact with primary and secondary host plant density and fragmentation to affect nascent *L. dispar* population growth at a landscape scale. In this study, we used a 16-year spatially-referenced dataset along the *L. dispar* expanding population front from Minnesota to North Carolina, USA, to quantify the role of temperature, and primary and secondary host plant density and distribution, on *L. dispar* population growth rates along its leading invasion front.

## Materials and Methods

### Study region

The spatial scale of this study encompassed the *L. dispar* invasion front within the United States from 1999 to 2015, which included an area from Minnesota to North Carolina. The invasion front was subset into three regions due to differences in regional range dynamics (Tobin et al. 2007b), temperature regimes (Gray 2004), and host plant availability (Morin et al., 2005). The Northern region consisted of Michigan, Wisconsin, and Minnesota; the Midwestern region consisted of Illinois, Indiana, and Ohio; and the Southern region consisted of North Carolina, Virginia, and West Virginia. To illustrate the differences in *L. dispar* spread by region, we estimated the year-to-year rate of *L. dispar* spread using boundary displacement (Sharov et al. 1996; Tobin et al. 2007a), and mean spread rates by region are presented in Table 1. Spread rates have been highest in the Northern region, lowest in the Midwestern region, and intermediate in the Southern region.

**Table 1** Mean ( $\pm$ SD) region-specific rates of *L. dispar* spread, and mean minimum January and mean maximum July temperatures, 1999–2015

| Region     | Rate of spread, km yr <sup>-1</sup> ( $\pm$ SD) | January minimum °C ( $\pm$ SD) | July maximum °C ( $\pm$ SD) |
|------------|---|--------------------------------|-----------------------------|
| Northern   | 14.8 (21.4)                                     | -7.3 (9.0)                     | 27.0 (1.7)                  |
| Midwestern | -2.7 (11.0)                                     | -1.1 (7.5)                     | 29.0 (2.0)                  |
| Southern   | 3.8 (10.9)                                      | 3.6 (5.9)                      | 30.1 (1.1)                  |

### *Lymantria dispar* growth rates

Growth rates were derived from monitoring data collected by the Slow-the-Spread program in which ~100,000 georeferenced pheromone-baited traps are deployed annually along and ahead of the *L. dispar* population front (Tobin et al. 2012). Pheromone-baited traps are generally deployed 2–8 km apart, with a finer resolution deployed in areas farthest from the established *L. dispar* area (Tobin et al. 2012). We used data from 1999–2015 as these years generally contained a continuous trap grid across the entire invasion front. Because some areas within the Slow-the-Spread program are treated for *L. dispar*, all traps within 1.5 km of a treated area were excluded; generally, <2% of the monitoring area is treated each year (Tobin et al. 2012). Because trap locations can shift from year-to-year, trap data (male moths/trap) from each year were interpolated using indicator kriging in GSLIB (Deutsch and Journel 1992) over a network of 5×5 km cells to generate a smooth surface (Sharov et al. 1995, 1997a). Within each region, we calculated growth rates for each 5×5 km cell. Because the Slow-the-Spread program monitors areas that are both along and ahead of the expanding population front, and our interest on newly establishing populations, we only used growth rates from cells at which there was an initial interpolated value >0 and <1 male moths/trap. To ensure growth rates within cells were comparable among cells through time and region, the data were further truncated to include cells that contained at least one value of 0 within the time sequence (1999–2015). We also estimated growth rates in cells with interpolated values from >0 and up to 10 male moths/trap. We used 10 as a threshold due to our interest in newly establishing *L. dispar* colonies given that 10 moths/trapping area is a benchmark used in the *L. dispar* Slow-the-Spread

program to denote *L. dispar* establishment and subsequent incorporation of the trapping area into the *L. dispar* federal quarantine (United States Department of Agriculture 2019). Growth rates from year  $t$  to  $t+1$  were calculated for each individual  $5 \times 5$  km cell and for each pair of years (e.g., 1999 to 2000, 2000 to 2001, ..., 2014 to 2015) according to:

$$\text{Growth Rate} = \log_e \left( \frac{N_{t+1}}{N_t} \right), \quad (1)$$

where  $N_t$  and  $N_{t+1}$  are the interpolated values (male moths/trap) in the current and following year, respectively.

### Temperature data

Temperature data were obtained through the PRISM Climate Group (2017). To represent the potential effect of suboptimal and supraoptimal temperatures for *L. dispar* development (Logan et al. 1991; Tobin et al. 2014a), we used mean daily minimum January and mean daily maximum July temperatures at a resolution of  $5 \times 5$  km for all years from 1999 to 2015 (PRISM Climate Group 2017), which we matched with the growth rate in the cell during the corresponding time period. For example, the growth rate in a cell from 1999 to 2000 was linked to the mean January minimum temperature in 2000 in this cell (to which overwintering eggs are subjected regardless of the region) and the mean July maximum temperature in 2000 in this cell (to which late instars-to-adults are subjected, depending on the region). Although we recognize that different *L. dispar* stages are present in July depending on the region, we used July maximum temperatures as a proxy for maximum summer heat. The mean minimum January temperature and mean maximum July temperature are summarized by region in Table 1.

### Host plant fragmentation

Forest inventory data were obtained from the U.S. Forest Service, Forest Inventory Analysis (2017) as an ArcGIS layer at a scale of  $240 \times 240$  m. These inventories are typically conducted every 5–15 years and include more than 1000 plots within each state on both private and federal lands. From this inventory, we quantified the proportion of basal area (e.g.,

the mean amount of an area occupied by tree stems, which is based upon stem diameter  $\sim 1.3$  m from the ground) attributed to each tree species within the study region. Tree species were classified as either primary or secondary host plants according to Liebhold et al. (1995). Common primary host tree genera in the study region included aspen (*Populus* spp.), birch (*Betula* spp.), hawthorn (*Crataegus* spp.), larch (*Larix* spp.), oak (*Quercus* spp), and willow (*Salix* spp). Common secondary host tree genera in the study region included beech (*Fagus* spp.), elm (*Ulmus* spp.), hickory (*Carya* spp.), maple (*Acer* spp.), pine (*Pinus* spp.), and walnut (*Juglans* spp.).

We used FRAGSTATS 3.3 (McGarigal et al. 2012) to estimate mean patch cohesion for primary and secondary host plants. Mean patch cohesion was estimated across a network of  $240 \times 240$  m cells that were fully contained into each  $5 \times 5$  km cell, which was linked to *L. dispar* growth rates. The patch cohesion index quantifies the connectivity of a specific host type patch within the entirety of the landscape. Patch cohesion increases as the host type patch becomes more aggregated within the landscape. This index will approach 0 as a host type becomes more fragmented, and approach 100 as a host type becomes less fragmented. Patch cohesion index, PCI, was estimated according to:

$$\text{PCI} = \left[ 1 - \frac{\sum_{j=1}^n P_{ij}}{\sum_{j=1}^n P_{ij} \sqrt{a_{ij}}} \right] \left[ 1 - \frac{1}{\sqrt{A}} \right]^{-1} \cdot (100), \quad (2)$$

where  $p_{ij}$  is the perimeter of patch  $ij$  in terms of the number of cell surfaces,  $a_{ij}$  is the area of patch in terms of the number of cells, and  $A$  is the total number of cells within the landscape.

### Statistical analyses

Due to spatial autocorrelation in *L. dispar* growth rates, which complicates data analysis due to the lack of independence, we sought to account for spatial autocorrelation in growth rates in our analyses. First, we estimated spatial autocorrelation in *L. dispar* growth rates in each region across the network of  $5 \times 5$  km cells for each pair of years from 1999 to 2015. We used the ncf package (Bjørnstad 2020) in R (Bjørnstad 2020; R Core Team 2018). Confidence intervals were estimated using the 2.5 and

97.5 percentiles of a bootstrapped distribution based on 300 replications (Efron and Tibshirani 1993). We also estimated spatial synchrony in *L. dispar* growth rates in each region using the *ncf* package (Bjørnstad 2020). Due to computation challenges given the spatial and temporal extent of the dataset (i.e., ~5000 cells for each of the 16 year-to-year pairs of growth rates), we randomly selected a subset of 500 locations through time for each region, from which we estimated spatial synchrony. This was repeated 5000 times to estimate a mean and confidence interval based on the 2.5 and 97.5 percentiles of the bootstrapped distribution. We then accounted for spatial autocorrelation in growth rates by including the distance-weighted mean of the growth rate as a term in our analyses according to Walter et al. (2015). Based on spatial autocorrelation of the growth rates (see results), cells in the Midwestern and Southern regions that were > 100 km apart were assigned a weight of 0. Within the Northern region, cells > 160 km apart were assigned a weight of 0. Otherwise, the weight,  $w_{ij}$ , was calculated based on the fitted relationship between spatial autocorrelation and distance in each region according to:

$$\text{Northern region : } w_{ij} = 6.7 - 0.54 \times \log_{10}(5.445 \times 10^{-4} + d_{ij}), \quad (3)$$

$$\text{Midwestern region : } w_{ij} = -0.16 - 0.94 \times \exp(-1.9 \times 10^{-5} + d_{ij}), \quad (4)$$

$$\text{Southern region : } w_{ij} = -0.044 - 0.51 \times \exp(-1.6 \times 10^{-5} + d_{ij}), \quad (5)$$

where  $d_{ij}$  is the straight-line distance between the focal points  $i$  and  $j$  (Anselin and Bera 1998). The distance-weighted mean growth rate,  $\bar{\lambda}_m$ , was then calculated as:

$$\bar{\lambda}_m = \frac{\sum_{j=1}^n w_{ij} \lambda_j}{\sum_{j=1}^n w_{ij}}, \quad (6)$$

where  $\lambda_j$  are the mean growth rates within the previously defined spatial autocorrelated neighborhood for each region (Walter et al. 2015).

In subsequent analyses, we use generalized additive models (GAMs). GAMs combine properties of generalized linear models and additive models,

allowing the replacement of linear regression coefficients with nonparametric smooth functions such as splines (Hastie and Tibshirani 1987). Using smoothed estimates for covariates is advantageous as it allows for the detection of nonlinear relationships, such as those between environmental covariates and aspects of *L. dispar* population dynamics (Haynes et al. 2012; Sharov et al. 1997b). In GAMs, smooth functions are penalized for increased nonlinearity to balance model fit and complexity. We used a backward selection protocol, based on Wood and Augustin (2002), to arrive at a parsimonious model for each region beginning with the following full model:

$$\begin{aligned} \lambda_m = & s(\bar{\lambda}_m) + s(\text{JanM}) + s(\text{JulM}) + s(\text{PrimeCoh}) \\ & + s(\text{SecCoh}) + s(\text{PrimeBA}) \\ & + s(\text{SecBA}) + te(\text{PrimeCoh}, \text{SecCoh}) \\ & + te(\text{SecBA}, \text{PrimeBA}) + te(\text{PrimeCoh}, \text{PrimeBA}) \\ & + te(\text{SecCoh}, \text{SecBA}) \end{aligned} \quad (7)$$

in which the growth rate,  $\lambda_m$ , was predicted by mean minimum January temperature (JanM), mean maximum July temperature (JulM), primary (Prime) and secondary (Sec) host cohesion (Coh) and basal area (BA), the distance-weighted mean growth rate ( $\bar{\lambda}_m$ ), and biologically important interaction effects. Within the full model,  $s$  indicates a smooth spline function of the covariates and  $te$  indicates a tensor product smooth. Following Wood and Augustin (2002), variables were removed from the model if: (1) the estimated degrees of freedom for that term were close to 1; (2) the confidence region for the smooth function included zero for all values of the independent variable; and (3) the generalized cross-validation (GCV) score for the full model decreases if the term is removed. GAMs were implemented using the *mgcv* package (Wood 2006) in R (R Core Team 2018).

## Results

Summary statistics on the mean *L. dispar* growth rate for each region are presented in Table 2. Overall mean growth rates (i.e., across all years) were highest in the Northern region and lowest in the Midwestern region. The highest and lowest year-to-year mean growth rate was observed from the Northern region, which was the region most likely to be subjected to

**Table 2** Region-specific *L. dispar* growth rates, 1999–2015

| Region     | Overall mean growth rate ( $\pm$ SD) | Maximum year-to-year growth rate | Minimum year-to-year growth rate | % of years with mean growth rate > 0 |
|------------|--------------------------------------|----------------------------------|----------------------------------|--------------------------------------|
| Northern   | 0.162 (1.346)                        | 2.678                            | −1.656                           | 50.0                                 |
| Midwestern | −0.026 (0.664)                       | 0.825                            | −1.244                           | 50.0                                 |
| Southern   | 0.127 (0.867)                        | 1.478                            | −1.456                           | 62.5                                 |

colder overwintering conditions (Table 1), including the 2014 North American cold wave during which the lowest year-to-year growth rate was observed.

We observed significant local spatial autocorrelation (i.e., the estimate of spatial autocorrelation as the lag distance approaches 0) in growth rates in all regions (Table 3), and spatial ranges that generally extended beyond 50 km (Metz 2017, Supplemental Information 1–3). We also observed spatial synchrony in growth rates in all regions (Fig. 1). In all regions, significant spatial synchrony (based on 95% confidence intervals) extended to at least 250 km, while synchrony in the northern region was measured to ~500 km. Statistical details of the GAM models testing the main and interaction effects on *L. dispar* growth rates (Eq. 7) for each region are presented in Table 4. The distance weighted mean growth rate, ( $\bar{\lambda}_m$ ), consistently met retention criteria and was retained in all GAM models, suggesting that its inclusion reduced spatial autocorrelation in the GAM residuals (Walter et al. 2015). This was not surprising given the extent to which growth rates were spatially autocorrelated (Table 3, Supplemental Information 1–3).

Mean minimum temperatures in January and mean maximum temperatures in July were retained in GAM models for all regions (Table 4). *Lymantria dispar* growth rates in all regions were highest when mean minimum January temperatures were > −10 °C (Fig. 2). In overwintering *L. dispar* eggs, mortality generally begins at ~−18 °C (Campbell 1973; Sullivan and Wallace 1972). Although mean January minimum temperatures were < −18 °C for only three years in the Northern region, we did observe reductions in growth rates when temperatures were < −18 °C (Fig. 2A). The optimal temperature for *L. dispar* larval development is ~28 °C (Casagrande et al. 1987; Logan et al. 1991). Although year-to-year growth rates, when summarized by region, are variable, the highest growth rates across all regions tended

to be observed at mean maximum July temperatures between 27 and 30 °C (Fig. 2B).

Excluding temperature, no other main or interaction effects significantly predicted growth rates in the Midwestern region. Also, the basal area of primary or secondary host species were not significant predictors of *L. dispar* growth rates in any region (Table 4). However, primary host species cohesion as a main effect, and its interaction with secondary host species cohesion, significantly predicted growth rates in the Southern region. Secondary host species cohesion as a main effect, and its interaction with primary host species cohesion, significantly predicted growth rates in the Northern region (Table 4). In the Northern and Southern regions, the results underscore the importance of host plant cohesion, as opposed to basal area per se, in the *L. dispar* invasion process.

In Southern region, primary host plants generally have a high degree of cohesion. However, we did observe increases in *L. dispar* growth rates as primary host plant cohesion increased. Moreover, when considering the significant interaction between primary host species cohesion and secondary host species cohesion (Table 4), estimates of growth rates in the Southern region were highest when primary and secondary host cohesion were > 80 (Fig. 3). In the Northern region, there was more variation in both primary and secondary host plant cohesion. When considering the significant interaction between primary host species cohesion and secondary host species cohesion in the Northern region (Table 4), *L. dispar* growth rates were highest when primary and secondary host cohesion were > 40. However, we also observed high *L. dispar* growth rates in areas with low primary host plant cohesion when secondary host plant cohesion, which was significant as a main effect in this region (Table 4), was > 30 (Fig. 3). The predicted overall *L. dispar* growth rates (1999–2015) when using region-specific GAM models that incorporate significant

**Table 3** Estimates ( $\pm 95\%$ ) bootstrapped confidence intervals) of the local spatial autocorrelation and spatial range (km) in the year-to-year growth rates across the Northern, Midwestern, and Southern regions of the *L. dispar* invasion front

| Years     | Northern                                  | Midwestern                                | Southern                                  |
|-----------|---|---|---|
|           | Local (95% CI)<br>Range (95% CI)          | Local (95% CI)<br>Range (95% CI)          | Local (95% CI)<br>Range (95% CI)          |
| 1999–2000 | 0.99 (0.93, 1.05)<br>156.1 (149.1, 162.8) | 0.99 (0.85, 1.18)<br>103.3 (97.4, 115.9)  | 0.83 (0.73, 0.92)<br>169.4 (146.4, 178.4) |
| 2000–2001 | 0.99 (0.83, 1.11)<br>127.6 (54.4, 131.5)  | 0.98 (0.83, 1.19)<br>93.4 (89.4, 98.1)    | 0.85 (0.77, 0.93)<br>327.2 (151.2, 332.2) |
| 2001–2002 | 0.97 (0.80, 1.10)<br>52.6 (49.4, 55.4)    | 0.96 (0.78, 1.23)<br>90.0 (78.9, 97.9)    | 0.65 (0.56, 0.72)<br>67.3 (61.8, 74.5)    |
| 2002–2003 | 0.96 (0.82, 1.06)<br>160.1 (64.1, 167.4)  | 0.67 (0.50, 0.84)<br>121.8 (113.3, 141.0) | 0.85 (0.76, 0.94)<br>221.8 (212.9, 233.4) |
| 2003–2004 | 0.97 (0.86, 1.07)<br>130.9 (126.4, 136.4) | 0.73 (0.54, 0.93)<br>113.0 (108.0, 119.9) | 0.79 (0.71, 0.87)<br>223.3 (169.4, 238.5) |
| 2004–2005 | 0.53 (0.45, 0.64)<br>147.7 (75.6, 162.2)  | 0.58 (0.41, 0.74)<br>85.2 (69.1, 93.9)    | 0.69 (0.59, 0.76)<br>113.4 (65.5, 122.7)  |
| 2005–2006 | 0.99 (0.93, 1.09)<br>160.7 (157.0, 164.1) | 0.65 (0.51, 0.78)<br>68.2 (54.1, 89.2)    | 0.72 (0.64, 0.81)<br>140.5 (133.7, 146.7) |
| 2006–2007 | 0.93 (0.78, 1.05)<br>151.4 (147.3, 155.1) | 0.99 (0.75, 1.24)<br>100.5 (90.5, 108.7)  | 0.74 (0.69, 0.79)<br>158.9 (153.4, 165.1) |
| 2007–2008 | 0.80 (0.71, 0.90)<br>149.2 (133.5, 156.5) | 0.74 (0.62, 0.85)<br>143.0 (105.7, 241.2) | 0.70 (0.65, 0.75)<br>193.1 (189.4, 197.7) |
| 2008–2009 | 0.99 (0.88, 1.06)<br>157.9 (147.5, 271.3) | 0.77 (0.61, 0.93)<br>91.6 (82.7, 121.7)   | 0.66 (0.57, 0.74)<br>184.7 (173.5, 196.0) |
| 2009–2010 | 0.92 (0.83, 1.02)<br>115.5 (109.8, 120.4) | 0.90 (0.70, 1.13)<br>110.7 (101.1, 126.1) | 0.57 (0.49, 0.64)<br>82.4 (76.6, 96.7)    |
| 2010–2011 | 0.77 (0.67, 0.91)<br>139.5 (131.5, 159.8) | 0.80 (0.72, 0.86)<br>116.0 (112.5, 119.6) | 0.54 (0.40, 0.67)<br>174.7 (96.8, 181.7)  |
| 2011–2012 | 0.88 (0.75, 1.03)<br>81.1 (77.0, 85.5)    | 0.65 (0.51, 0.79)<br>204.4 (102.7, 210.2) | 0.69 (0.60, 0.77)<br>216.5 (160.9, 281.6) |
| 2012–2013 | 0.76 (0.69, 0.86)<br>283.3 (155.3, 294.0) | 0.81 (0.69, 0.94)<br>122.8 (113.0, 141.6) | 0.93 (0.82, 1.05)<br>142.3 (139.1, 146.7) |
| 2013–2014 | 0.88 (0.78, 0.95)<br>285.0 (168.0, 335.2) | 0.79 (0.65, 0.92)<br>144.8 (124.2, 150.9) | 0.90 (0.74, 1.03)<br>75.6 (68.4, 87.7)    |
| 2014–2015 | 0.85 (0.75, 0.97)<br>239.4 (212.9, 269.7) | 0.76 (0.64, 0.86)<br>180.4 (165.9, 204.7) | 0.85 (0.73, 0.96)<br>99.1 (92.3, 116.8)   |

predictors (Table 4) are shown in Fig. 4 along with the overall observed *L. dispar* growth rates.

## Discussion

Across the *L. dispar* expanding population front, the results reinforce the importance of temperature on *L. dispar* population growth. *Lymantria dispar* growth rates were maximized when mean July temperatures were between 27 and 30 °C. This is consistent with prior research in which exposure to supraoptimal temperatures has been found to affect larval development and survival, and spread rates (Thompson et al.

2017; Tobin et al. 2014a). This study also extends our understanding of the effect of cold temperatures on *L. dispar* population growth rates across a spatially-large and diverse landscape. The highest *L. dispar* growth rates were observed when mean minimum January temperatures were  $> -10$  °C (Fig. 2), which is consistent with previous research on *L. dispar* egg mass mortality at cold temperatures (Sullivan and Wallace 1972; Summers 1922). There were only three years in which minimum January temperatures were  $< -18$  °C, and all from the Northern region; however, it does demonstrate the constraining effect that overwintering temperatures can have on an invading species, even in a region where spread rates

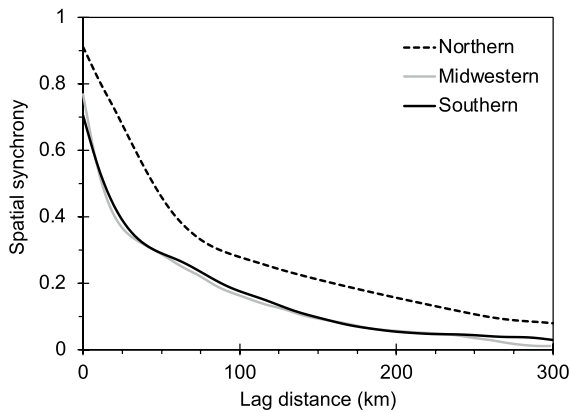


**Fig. 1** Estimates of spatial synchrony (Bjørnstad 2020) in *L. dispar* growth rates from the Northern, Midwestern, and Southern regions, 1999–2015

(Table 1) and growth rates (Table 2) are the highest along the invasion front. Given this constraint, warming winter temperatures in the Northern region would likely further increase *L. dispar* population growth

rates and invasion speed. Indeed, recent studies have reported *L. dispar* invasion success in northern Minnesota (Streifel et al. 2019; Tobin et al. 2016), which was previously considered to be climatically unsuitable to *L. dispar*, in part due to historical suboptimal winter temperatures (Gray 2004).

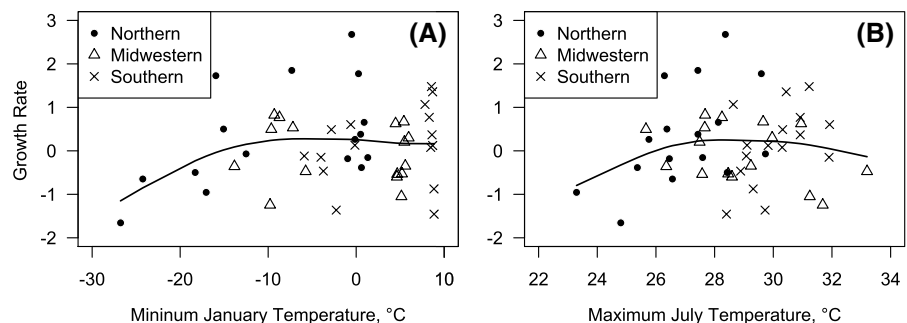
The high degree of spatial autocorrelation in *L. dispar* growth rates (Table 3) is not surprising given that insect populations tend to be highly spatially autocorrelated. It also underscores the importance of considering spatial autocorrelation when assessing the factors that affect *L. dispar* growth rates, and when developing predictive models of invasion across a landscape. When using the GAM modeling framework that incorporated distance weighted mean growth rates, we determined that *L. dispar* growth rates in the Midwestern region were driven by temperature only (Table 4). This region contains a low density of *L. dispar* primary host plants and forest cover, with little variation in the density of each (Morin et al. 2005), which may have reduced the predictive capability of primary host density and

**Table 4** Results of the GAM models predicting *L. dispar* moth growth rates (Eq. 7) in the Southern, Midwestern, and Northern regions (estimated degrees of freedom for each pre-

dictor variable is noted in parentheses). All main effects are shown, but only significant interaction terms are listed

| Predictor variable                | Southern region             | Midwestern region           | Northern region             |
|-----------------------------------|-----------------------------|-----------------------------|-----------------------------|
| $\bar{\lambda}_m$                 | F = 168.0 (8.6); $P < 0.01$ | F = 172.0 (8.3); $P < 0.01$ | F = 177.0 (8.4); $P < 0.01$ |
| Mean January minimum              | F = 2.1 (8.7); $P = 0.02$   | F = 2.3 (4.1); $P = 0.03$   | F = 14.0 (6.8); $P < 0.01$  |
| Mean July maximum                 | F = 8.2 (8.5); $P < 0.01$   | F = 2.7 (7.3); $P < 0.01$   | F = 3.8 (5.8); $P < 0.01$   |
| Primary host basal area           | NS                          | NS                          | NS                          |
| Secondary host basal area         | NS                          | NS                          | NS                          |
| Primary host cohesion             | F = 7.1 (4.2); $P < 0.01$   | NS                          | NS                          |
| Secondary host cohesion           | NS                          | NS                          | F = 3.6 (4.8); $P < 0.01$   |
| Primary × Secondary host cohesion | F = 7.4 (3.1); $P < 0.01$   | NS                          | F = 3.1 (10.0); $P < 0.01$  |

**Fig. 2** Region-specific mean *L. dispar* growth rates by mean minimum January **A** and mean maximum July **B** temperature for each pair of years (e.g., 1999–2000, .... 2014–2015). Fitted lines are estimated using locally-weighted polynomial regression





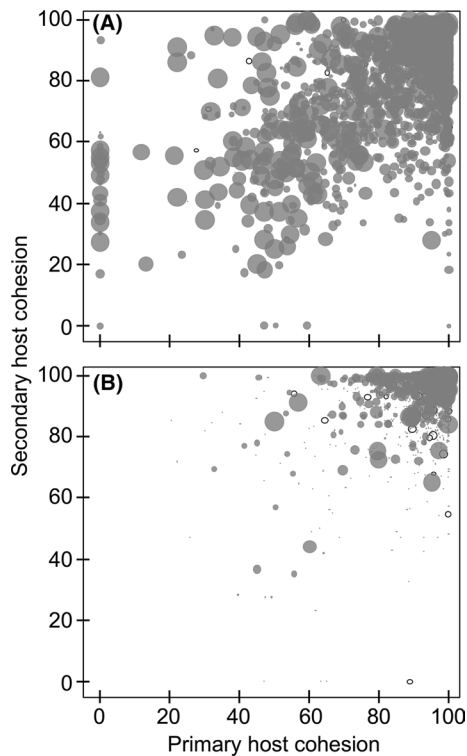


**Fig. 3** Relationship between primary and secondary host species cohesion, and mean *L. dispar* growth rates in the Northern **A** and Southern **B** regions. Mean growth rates were averaged across all years (1999–2015). The size of the circles is proportional to the growth rate; the largest-sized circles represent growth rates  $\geq 2$  or  $\leq -2$ , and the smallest sized circles are 0. Grey circles are positive growth rates and open circles are negative growth rates

cohesion on *L. dispar* growth rates. Instead, growth rates appear to be mostly affected by both overwintering temperatures and temperatures during larval feeding. Specifically, low temperatures in January below  $-10$  °C and high temperatures in July above the optimal temperature for immature development ( $28$  °C) would decrease the growth rates in this region.

In contrast to the Midwestern region, the Southern region contains a high density of *L. dispar* primary host plants and a high density of forest cover, especially in the Appalachian Mountains (Morin et al. 2005). The fact that primary host basal area did not statistically predict *L. dispar* growth rates is perhaps due to large-scale availability of primary host plants throughout this region. Instead, primary host plant cohesion was a significant predictor

of growth rates in this region, with growth rates increasing in areas where primary hosts are less fragmented (Fig. 3). There was also an interaction with secondary host plants in this region (Table 4), with higher predicted growth rates in areas that also have high secondary host plant cohesion (Fig. 3). Temperatures during January and July are also important predictors of *L. dispar* growth rates in the Southern region, and past research has reported that supraoptimal temperatures during larval development causes range retraction in portions of this region (Tobin et al. 2014a).

The Northern region contains areas of relatively high amounts of *L. dispar* primary host plants and forest cover, especially in its northern portions, and areas with very low amounts of *L. dispar* primary host plants and forest cover, especially in its southern portions (Morin et al. 2005). In this region, we detected an effect of secondary host plant cohesion, and its interaction with primary host plants (Table 4). Growth rates in this region were higher when the cohesion of both primary and secondary hosts increased (Fig. 3). However, in the absence of high primary host cohesion, *L. dispar* growth rates were  $\geq 2$  provided that secondary host cohesion was  $> 40$ . The presence of high secondary host cohesion could reflect the availability of *L. dispar* host plants that can sustain populations, even if these plants are not classified as preferred host species. It could also reflect higher forest cover and therefore, an increased potential for available host plants. Lastly, the classification of host plants as primary or secondary, according to Liebhold et al. (1995), is useful but is also a broad classification that does not consider variation within primary or secondary classifications. Some plants classified as primary hosts, such as *Quercus* spp., could be more suitable to *L. dispar* larvae than others, such as *Betula* and *Populus* spp., that are also classified as primary hosts. Similarly, there is variation in plants classified as secondary hosts, with some hosts (*Acer* spp.) more suitable than others (*Carya* spp.). The results from the Northern region, where primary hosts are in abundance in some areas and in paucity in others, suggest that secondary host plants can be important in maintaining *L. dispar* populations when primary hosts are scarce.

The spread of non-native insect species often occurs through stratified dispersal in which colonies are formed ahead of an expanding population front

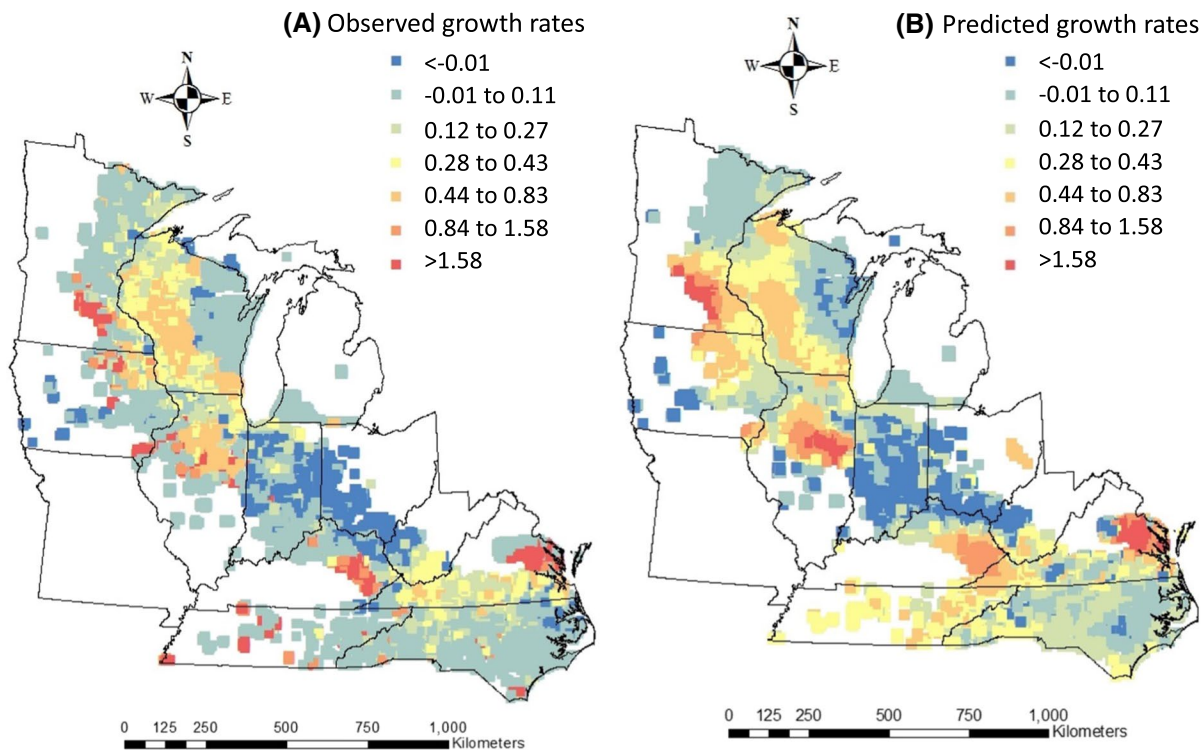


**Fig. 4** Observed **A** and predicted **B** spatially-explicit mean *L. dispar* growth rates, 1999–2015. Predicted growth rates are derived from region-specific GAM models that incorporate temperature, and when applicable to the region, primary and secondary host plant cohesion (Table 4). Observed and predicted growth rates from some states are shown even though

they were not included in the analysis (i.e., Iowa, Kentucky, and Tennessee); data from these states were excluded due to limited spatial and temporal extent of *L. dispar* monitoring. Predictions in Kentucky and Tennessee were based on the Southern region GAM model, and predictions in Iowa were based on the Midwestern region GAM model

(Shigesada et al. 1995; Liebhold and Tobin 2008). For invading insect herbivores, the presence of suitable host plants is a necessity for successful population establishment and growth in newly-arriving colonies. Not surprisingly, host plant availability is a key ingredient in risk models to predict establishment (Venette 2015). Temperature also poses a barrier to invading insect species, which have species-specific tolerances to extreme hot and cold temperatures; consequently, climate suitability models are also used to predict invasive insect distributions (Venette 2017). Incorporating temperature constraints (Gray 2004; Logan et al. 2007; Pitt et al. 2007) and the distribution of primary host species (Morin et al. 2005) into *L. dispar* risk models is not new. However, we provide evidence that host plant cohesion, as opposed to host basal area, predicts *L. dispar* growth rates in new populations along its expanding population front. Including host plant cohesion as a factor in risk

models, either in addition to or in place of host plant density, could improve the predictive capability of risk assessment models in other invading herbivorous insect species.

**Acknowledgements** We are grateful to Drs. L. Monika Moscal and Jonathan Bakker (University of Washington) for reviewing an earlier draft of this manuscript. We would like to acknowledge financial support from USDA Farm Bill Section 10007 (Cooperator Agreement No. A112430 to PCT), the National Science Foundation (DEB-1556111 to PCT), and the University of Washington. This research was conducted by RM in partial fulfillment of the requirements for the M.S. degree from the University of Washington.

**Author contributions** RM: Conceptualization, Investigation, Analysis, Writing; PCT: Conceptualization, Analysis, Funding acquisition, Project administration, Writing.

**Funding** National Science Foundation, USDA.

**Data availability** Data available through ResearchWorks at the University of Washington.

**Code availability** Not applicable.

### Declarations

**Conflict of interest** The authors declare no conflict of interest.

**Ethical approval** Not applicable.

**Consent to participate** Not applicable.

**Consent for publication** Not applicable.

### References

- Allen JC, Foltz JL, Dixon WN et al (1993) Will the gypsy moth become a pest in Florida? *Fla Entomol* 76:102–113
- Bale JS, Masters GJ, Hodkinson ID et al (2002) Herbivory in global climate change research: direct effects of rising temperature on insect herbivores. *Glob Change Biol* 8:1–16
- Barbosa P, Greenblatt J (1979) Suitability, digestibility and assimilation of various host plants of the gypsy moth *Lymantria dispar* L. *Oecologia* 43:111–119
- Barbosa P, Krischik VA (1987) Influence of alkaloids on feeding preference of eastern deciduous forest trees by the gypsy moth *Lymantria dispar*. *Am Nat* 130:53–69
- Biggsby KM, Tobin PC, Sills EO (2011) Anthropogenic drivers of gypsy moth spread. *Biol Invasions* 13:2077–2090
- Bjørnstad ON (2020) Package 'ncf.' Spatial nonparametric covariance functions. Available at: <http://cran.r-project.org/web/packages/ncf/>
- Campbell RW (1973) Numerical behavior of a gypsy moth population system. *For Sci* 19:162–167
- Casagrande RA, Logan PA, Wallner WE (1987) Phenological model for gypsy moth, *Lymantria dispar* (Lepidoptera: Lymantriidae), larvae and pupae. *Environ Entomol* 16:556–562
- Collinge SK (2000) Effects of grassland fragmentation on insect species loss, colonization, and movement patterns. *Ecology* 81:2211–2226
- Connor EF, Courtney AC, Yoder JM (2000) Individuals-area relationships: the relationship between animal population density and area. *Ecology* 81:734–748
- Contarini M, Onufrieva KS, Thorpe KW et al (2009) Mating failure as an important cause of Allee effects along the leading edge of an invading insect population. *Entomol Exp Appl* 133:307–314
- Cronin JT (2003) Movement and spatial population structure of a prairie planthopper. *Ecology* 84:1179–1188
- Denno RF, Raupp MJ, Tallamy DW (1981) Organization of a guild of sap-feeding insects: equilibrium vs. nonequilibrium coexistence. Springer New York, New York, NY, pp 151–181
- Deutsch CV, Journel AG (1992) GSLIB: geostatistical software library and user's guide. Oxford University Press, New York
- Doane CC, McManus ML (1981) The gypsy moth: research toward integrated pest management. Technical Bulletin 1584, United States Department of Agriculture, Washington, D.C.
- Efron B, Tibshirani RJ (1993) An introduction to the bootstrap. Chapman & Hall, London
- Elkinton JS, Liebhold AM (1990) Population dynamics of gypsy moth in North America. *Annu Rev Entomol* 35:571–596
- Esper J, Büntgen U, Frank DC et al (2007) 1200 years of regular outbreaks in alpine insects. *Proc R Soc Biol Sci Ser B* 274:671–679
- Gray DR (2004) The gypsy moth life stage model: landscape-wide estimates of gypsy moth establishment using a multi-generational phenology model. *Ecol Model* 176:155–171
- Gray DR (2009) Age-dependent postdiapause development in the gypsy moth (Lepidoptera: Lymantriidae) life stage model. *Environ Entomol* 38:18–25
- Grayson KL, Johnson DM (2018) Novel insights on population and range edge dynamics using an unparalleled spatiotemporal record of species invasion. *J Anim Ecol* 87:581–593
- Hajek AE, Tobin PC (2009) North American eradications of Asian and European gypsy moth. In: Hajek AE, Glare TR, O'Callaghan M (eds) Use of microbes for control and eradication of invasive arthropods. Springer, New York, pp 71–89
- Hanski I (1998) Metapopulation dynamics. *Nature (Lond)* 396:41–49
- Hanski I, Gilpin M (1991) Metapopulation dynamics: brief history and conceptual domain. *Biol J Linn Soc* 42:3–16
- Hastie T, Tibshirani R (1987) Generalized additive models: some applications. *J Am Stat Assoc* 82:371–386
- Haynes KJ, Allstadt AJ, Klimetzek D (2014) Forest defoliator outbreaks under climate change: effects on the frequency and severity of outbreaks of five pine insect pests. *Glob Change Biol* 20:2004–2018
- Haynes KJ, Liebhold AM, Johnson DM (2009) Spatial analysis of harmonic oscillation of gypsy moth outbreak intensity. *Oecologia* 159:249–256
- Haynes KJ, Liebhold AM, Johnson DM (2012) Elevational gradient in the cyclicity of a forest-defoliating insect. *Popul Ecol* 54:239–250
- Hengeveld R (1989) Dynamics of biological invasions. Chapman and Hall, London, UK
- Herrick OW, Gansner DA (1986) Rating forest stands for gypsy moth defoliation. USDA Forest Service Research Paper NE-583, Broomall, PA
- Hill JK, Griffiths HM, Thomas CD (2011) Climate change and evolutionary adaptations at species' range margins. *Annu Rev Entomol* 56:143–159
- Hunter MD (2002) Landscape structure, habitat fragmentation, and the ecology of insects. *Agric for Entomol* 4:159–166
- Jepsen JU, Hagen SB, Ims RA et al (2008) Climate change and outbreaks of the geometrids *Operophtera brumata* and *Epipirrita autumnata* in subarctic birch forest: evidence of a recent outbreak range expansion. *J Anim Ecol* 77:257–264

- Johnson DM, Liebhold AM, Tobin PC et al (2006) Allee effects and pulsed invasion of the gypsy moth. *Nature* 444:361–363
- Liebhold AM, Elmes GA, Halverson JA et al (1994) Landscape characterization of forest susceptibility of gypsy moth defoliation. *For Sci* 40:18–29
- Liebhold AM, Gottschalk KW, Muzika RM, et al. (1995) Suitability of North American tree species to the gypsy moth: a summary of field and laboratory tests. USDA Forest Service General Technical Report NE-211, Radnor, PA
- Liebhold AM, Halverson JA, Elmes GA (1992) Gypsy moth invasion in North America: a quantitative analysis. *J Biogeogr* 19:513–520
- Liebhold AM, Tobin PC (2006) Growth of newly established alien populations: comparison of North American gypsy moth colonies with invasion theory. *Popul Ecol* 48:253–262
- Liebhold AM, Tobin PC (2008) Population ecology of insect invasions and their management. *Annu Rev Entomol* 53:387–408
- Logan JA, Casagrande RA, Liebhold AM (1991) Modeling environment for simulation of gypsy moth (Lepidoptera: Lymantriidae) larval phenology. *Environ Entomol* 20:1516–1525
- Logan JA, Régnière J, Gray DR et al (2007) Risk assessment in face of a changing environment: gypsy moth and climate change in Utah. *Ecol Appl* 17:101–117
- Logan JA, Régnière J, Powell JA (2003) Assessing the impacts of global warming on forest pest dynamics. *Front Ecol Environ* 1:130–137
- McGarigal K, Cushman SA, Ene E (2012) FRAGSTATS v4: Spatial pattern analysis program for categorical and continuous maps. Computer software program produced by the authors at the University of Massachusetts, Amherst. Available at: <http://www.umass.edu/landeco/research/fragstats/fragstats.html>
- Metz R (2017) Effects of temperature and host distribution on gypsy moth growth rates along its expanding population front. M.S. Thesis, University of Washington, Seattle, WA
- Miller JS, Feeny P (1983) Effects of benzylisoquinoline alkaloids on the larvae of polyphagous Lepidoptera. *Oecologia* 58:332–339
- Morin RS, Liebhold AM, Luzader ER, et al. (2005) Mapping host-species abundance of three major exotic forest pests. USDA Forest Service Research Paper NE-726, Newtown Square, PA
- Pitt JPW, Régnière J, Worner S (2007) Risk assessment of the gypsy moth, *Lymantria dispar* (L.), in New Zealand based on phenology modelling. *Int J Biometeorol* 51:295–305
- PRISM Climate Group (2017) Oregon State University. Available at: <http://prism.oregonstate.edu>
- R Core Team (2018) R: A Language and Environment for Statistical Computing, R Foundation for Statistical Computing, Vienna, Austria. Available at: <http://www.R-project.org/>
- Sharov AA, Roberts EA, Liebhold AM, Ravlin FW (1995) Gypsy moth (Lepidoptera: Lymantriidae) spread in the central Appalachians: three methods for species boundary estimation. *Environ Entomol* 24:1529–1538
- Sharov AA, Liebhold AM, Roberts EA (1996) Spread of gypsy moth (Lepidoptera: Lymantriidae) in the central Appalachians: comparison of population boundaries obtained from male moth capture, egg mass counts, and defoliation records. *Environ Entomol* 25:783–792
- Sharov AA, Liebhold AM, Roberts EA (1997a) Methods for monitoring the spread of gypsy moth (Lepidoptera: Lymantriidae) populations in the Appalachian Mountains. *J Econ Entomol* 90:1259–1266
- Sharov AA, Liebhold AM, Roberts EA (1997b) Correlation of counts of gypsy moths (Lepidoptera: Lymantriidae) in pheromone traps with landscape characteristics. *For Sci* 43:483–490
- Sharpe PJH, DeMichele DW (1977) Reaction kinetics of poikilotherm development. *J Theor Biol* 64:649–670
- Shigesada N, Kawasaki K, Takeda Y (1995) Modeling stratified diffusion in biological invasions. *Am Nat* 146:229–251
- Stoyenoff JL, Witter JA, Montgomery ME et al (1994) Effects of host switching on gypsy moth (*Lymantria dispar* (L.)) under field conditions. *Oecologia* 97:143–157
- Streifel M, Tobin PC, Kees AM et al (2019) Range expansion of *Lymantria dispar dispar* (L.) (Lepidoptera: Erebidae) along its north-western margin in North America despite low predicted climatic suitability. *J Biogeogr* 46:58–69
- Sullivan CR, Wallace DR (1972) The potential northern dispersal of the gypsy moth, *Porthetria dispar*. *Can Entomol* 104:1349–1355
- Summers JN (1922) Effect of low temperatures on the hatching of gypsy moth eggs. U.S. Department of Agriculture Bulletin 1080:1–14
- Tauber MJ, Tauber CA, Masaki S (1986) Seasonal adaptations of insects. Oxford University Press, New York, NY
- Thompson LM, Fiske TM, Banahene N et al (2017) Variation in growth and developmental responses to supraoptimal temperatures near latitudinal range limits of gypsy moth *Lymantria dispar* (L.), an expanding invasive species. *Physiol Entomol* 42:181–190
- Tobin PC, Bai BB, Eggen DA et al (2012) The ecology, geopolitics, and economics of managing *Lymantria dispar* in the United States. *Int J Pest Manag* 53:195–210
- Tobin PC, Blackburn LM (2007) Slow the spread: a national program to manage the gypsy moth. USDA Forest Service General Technical Report NRS-6, Newtown Square, PA
- Tobin PC, Cremers KT, Hunt L et al (2016) All quiet on the western front? Using phenological inference to detect the presence of a latent gypsy moth invasion in Northern Minnesota. *Biol Invasions* 18:3561–3573
- Tobin PC, Gray DR, Liebhold AM (2014a) Supraoptimal temperatures influence the range dynamics of a non-native insect. *Divers Distrib* 20:813–823
- Tobin PC, Liebhold AM, Roberts EA (2007a) Comparison of methods for estimating the spread of a non-indigenous species. *J Biogeogr* 34:305–312
- Tobin PC, Parry D, Aukema BH (2014b) The influence of climate change on insect invasions in temperate forest ecosystems. In: Fenning T (ed) Challenges and opportunities for the World's Forests in the 21st Century. Springer, pp 267–296
- Tobin PC, Whitmire SL, Johnson DM et al (2007b) Invasion speed is affected by geographic variation in the strength of Allee effects. *Ecol Lett* 10:36–43
- United States Department of Agriculture (2019) Gypsy Moth Program Manual. Available at: <https://www.aphis.usda>

- [gov/import\\_export/plants/manuals/domestic/downloads/gypsy\\_moth.pdf](#)
- USDA Forest Service (2017) Forest Inventory Analysis. Available at: <https://www.fia.fs.fed.us/>.
- Venette RC (Ed.) (2015) Pest risk modelling and mapping for invasive alien species. Centre for Agriculture and Bioscience International, Wallingford.
- Venette RC (2017) Climate analyses to assess risks from invasive forest insects: simple matching to advanced models. *Current For Rep* 3:255–268
- Walter JA, Meixler MS, Mueller T et al (2015) How topography induces reproductive asynchrony and alters gypsy moth invasion dynamics. *J Anim Ecol* 84:188–198
- Weed AS, Ayres MP, Hicke JA (2013) Consequences of climate change for biotic disturbances in North American forests. *Ecol Monogr* 83:441–470
- Wood SN (2006) Generalized additive models: an introduction with R. Chapman and Hall/CRC, Boca Raton, FL
- Wood SN, Augustin NH (2002) GAMs with integrated model selection using penalized regression splines and applications to environmental modelling. *Ecol Model* 157:157–177

**Publisher's Note** Springer Nature remains neutral with regard to jurisdictional claims in published maps and institutional affiliations.